

# Development of a Thermoelectric Module Suitable for Vehicles and Based on $\text{CoSb}_3$ Manufactured Close to Production

MIRKO KLEIN ALTSTEDDE,<sup>1,4</sup> REINHARD SOTTONG,<sup>2</sup>  
OLIVER FREITAG,<sup>3</sup> MARTIN KOBER,<sup>1</sup> VOLKER DREIßIGACKER,<sup>3</sup>  
KNUD ZABROCKI,<sup>2</sup> and PATRIC SZABO<sup>3</sup>

1.—German Aerospace Center (DLR), Institute of Vehicle Concepts, Pfaffenwaldring 38-40, 70569 Stuttgart, Germany. 2.—German Aerospace Center (DLR), Institute of Materials Research, Linder Höhe, 51147 Köln, Germany. 3.—German Aerospace Center (DLR), Institute of Engineering Thermodynamics, Pfaffenwaldring 38-40, 70569 Stuttgart, Germany. 4.—e-mail: mirko.kleinaltstedde@dlr.de

Despite the ongoing electrification of vehicle propulsion systems, vehicles with combustion engines will continue to bear the brunt of passenger services worldwide for the next few decades. As a result, the German Aerospace Center Institute of Vehicle Concepts, the Institute of Materials Research and the Institute of Technical Thermodynamics have focused on utilising the exhaust heat of internal combustion engines by means of thermoelectric generators (TEGs). Their primary goal is the development of cost-efficient TEGs with long-term stability and maximised energy yield. In addition to the overall TEG system design, the development of long-term stable, efficient thermoelectric modules (TEMs) for high-temperature applications is a great challenge. This paper presents the results of internal development work and reveals an expedient module design for use in TEGs suitable for vehicles. The TEM requirements identified, which were obtained by means of experiments on the test vehicle and test bench, are described first. Doped semiconductor materials were produced and characterised by production methods capable of being scaled up in order to represent series application. The results in terms of thermoelectric properties (Seebeck coefficient, electrical conductivity and thermal conductivity) were used for the simulative design of a thermoelectric module using a constant-property model and with the aid of FEM calculations. Thermomechanical calculations of material stability were carried out in addition to the TEM's thermodynamic and thermoelectric design. The film sequence within the module represented a special challenge. Multilayer films facilitated adaptation of the thermal and mechanical properties of plasma-sprayed films. A joint which dispenses with solder additives was also possible using multilayer films. The research resulted in a functionally-optimised module design, which was enhanced for use in motor vehicles using process flexibility and close-to-production manufacturing methods.

**Key words:** Thermoelectric module, thermoelectric generator, waste heat recovery, thermomechanics

## INTRODUCTION/MOTIVATION

Besides aerospace research, the German Aerospace Center (DLR) also conducts in-depth research

in the fields of traffic and transport. This research is being conducted by collecting, processing and coordinating traffic-related content and topics, especially those involving vehicle design and automotive technologies. One area of interest is the increase in powertrain efficiency in future passenger and light duty vehicles by using advanced

---

(Received July 4, 2014; accepted November 6, 2014)

technologies in the area of alternative energy conversion.

A trend towards electrified and hybrid powertrain concepts has emerged in the development of motor vehicles for passenger transportation. However, current studies have shown that combustion engines will bear the brunt of non-urban traffic loads in particular.<sup>1</sup> The demand for concepts using secondary energy has increased significantly, driven by the demand for lower fuel consumption and lower emissions of polluting gases. In this case, the technology of using exhaust heat thermoelectrically through a thermoelectric generator (TEG) increasingly meets the requirements for higher efficiency demanded of internal combustion engine powertrains.<sup>2–4</sup> The gasoline engine's circular process creates exhaust heat, which is converted directly into electric energy. It is possible to relieve the alternator by feeding the electrical energy produced into the electrical supply system of the vehicle, thereby increasing fuel efficiency by nearly 3%<sup>5</sup> and cutting gas emissions.

In addition to overall TEG system design, the development of long-term stable, efficient thermoelectric modules (TEMs) for high-temperature applications is a great challenge.<sup>6–8</sup> This paper presents the results of internal development work and reveals a practical module design for use in TEGs suitable for vehicles.

## VEHICLE-SPECIFIC BOUNDARY CONDITIONS

### Thermodynamic Exhaust Gas Behavior

“Driving cycles” are used for the objective assessment of fuel consumption and the emission of pollutants by motor vehicles. A driving cycle defines a function of the vehicle speed throughout the journey time with vehicle-specific tractive resistance. The New European Driving Cycle (NEDC) has been used in Europe since 1996.

In future, it will be replaced by the Worldwide Harmonised Light Test Procedure (WLTP), which displays higher driving dynamics than the NEDC, in order to reflect reality more closely. Parameters for the use of TEGs appropriate for the vehicle can be derived directly from the conditions from the respective driving cycle.

The exhaust conditions have the greatest effect on TEG and TEM design, with the time curve of the exhaust gas temperature and the time curve of the exhaust gas mass flow constituting crucial design parameters. They are highly vehicle-specific and also display transient behaviour throughout the driving cycle.<sup>9</sup>

Operationally, however, heat exchangers can only reach their maximum efficiency at one design point, so the TEG cannot use the entire exergy available if the exhaust gas conditions deviate. In Fig. 1, the exergetic potential theoretically available at a design point (mass flow and temperature) throughout the WLTP has been plotted. The reference vehicle was an Audi A6 2.0 TFSI Hybrid.

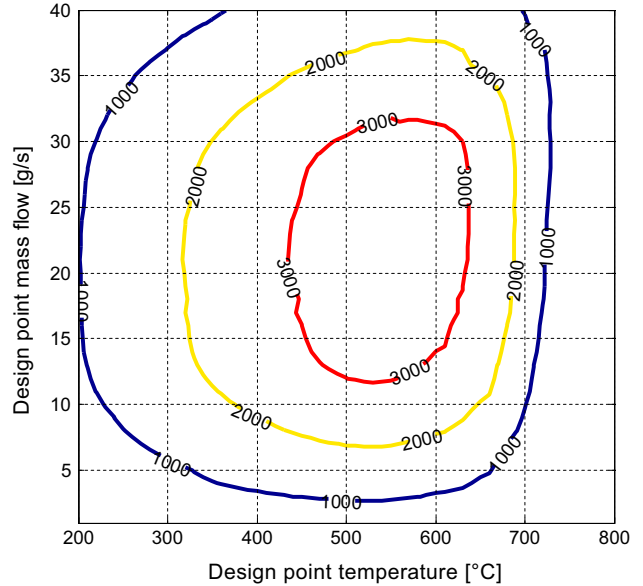


Fig. 1. Exergetic exhaust potential in kJ throughout the WLTP with variations in the Audi A6 2.0 TFSI Hybrid heat exchanger design parameters.

It is clearly evident that the maximum amount of energy of approximately 3000 kJ can be anticipated in a design range of about 12–32 g/s exhaust gas mass flow and about 430–630°C exhaust gas temperature. The TEG design points for differing exhaust gas conditions would have considerably less exergy available. Thermoelectric converter materials to cover the above-mentioned temperature range are therefore absolutely necessary from an exergetic point of view.

Systemic consideration of the vehicle now makes it possible to define the ideal design point, where negative influences on subsystems such as the cooling system and auxiliary units, and the costs of the TEG, are reduced to a minimum.

Not only the absolute design and operating temperatures of the TEG but also the alternating thermal load of the hot side of the module have a great effect on the long-term stability of the TEM. As an example, Fig. 2 shows plots of the temperature gradient (top) and the exhaust gas mass flow (bottom) over a period of 50 s in the WLTP. The reference vehicle remains the above-mentioned Audi.

The upper diagram shows that a maximum temperature gradient of approximately 70 K/s was measured on the exhaust gas side. It is attributable to the high engine dynamics of the reference vehicle examined and the gradients of the exhaust gas mass flow derived from them (lower diagram). Constant alternation between high engine loads and engine cut-off takes place throughout the driving cycle, due to the hybrid design of the powertrain.

The above statements show that, firstly, exhaust gas exergy is available at a high temperature level for thermoelectric conversion, and, secondly, that the temperature gradients (attributable to

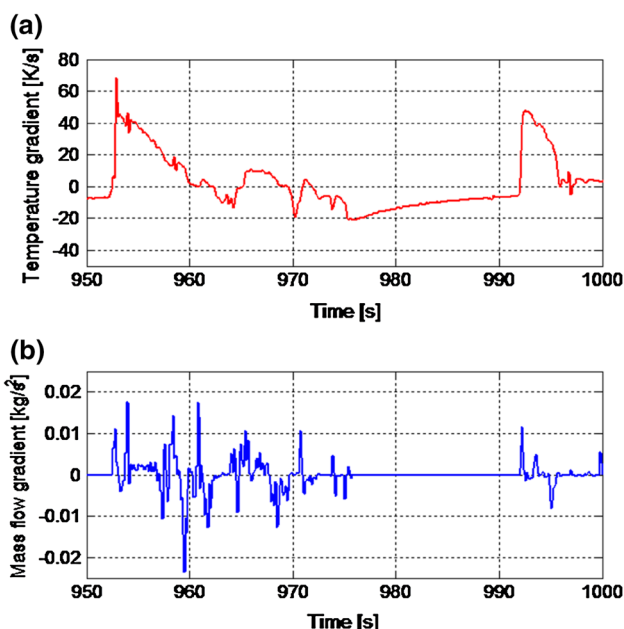


Fig. 2. (a) Exemplary flue gas temperature gradient, (b) flue gas mass flow gradient against driving time of an Audi A6 2.0 TFSI Hybrid.

hybridised powertrains) causes high alternating thermomechanical loads on the modules.

### Design Requirements Attributable to Automotive TEG Design

Three fundamental types of TEG structure may be distinguished for vehicular use: planar, hexagonal and round. Systemic analysis have revealed that the planar structure is the most promising in terms of production costs, power output (density) and component costs.<sup>5</sup> The planar TEM structure has been adopted as the development objective for this reason.

In the thermal design of a TEG, the hot gas heat exchanger is designed so that the hot side temperature is as high as possible. This is necessary because of the higher degree of efficiency at high temperatures. The maximum hot side temperature of the TEM then reaches up to 550°C in the test cycle. Another point to be considered in the design of the hot gas heat exchanger is the decrease of temperature in the longitudinal direction. The hot side temperature reached at the thermoelectric module decreases due to the cooling of the exhaust gases in the direction of flow. This can be countered by specific adaptation of the heat exchanger, but a decrease of temperature will ultimately be observed on the TEM in the direction of flow of the exhaust gases. An elongated module design is preferred for TEGs suitable for vehicles, to reduce their effect on the electrical power output.

As indicated in Fig. 3, the latter are at right angles to the exhaust gas flow. By using this design, TEMs operating at the same temperature level can

be connected electrically and their energy yield optimised block by block by means of maximum power point tracking (MPPT). Firstly, the electrical circuit reduces the MPPT outlay and secondly each module block can be operated at its individual optimum power.

### $\text{CoSb}_3$ Manufactured Close to Production

The use of thermoelectric generators in vehicles demands high availability of highly-efficient *p*- and *n*-doped thermoelectric semiconductors with long-term thermal and mechanical stability. Skutterudite materials are expected to provide these properties for the given temperature conditions at low cost.<sup>10</sup> These semiconductors were fabricated at DLR using the gas atomisation technique which produces fine-grain powders from a melt by dispersing the material using a gas stream. This process provides material on a scale of kilograms at DLR and can be scaled up to the amounts of material necessary for series production of TEGs. Figure 4 shows the production facility used at DLR for thermoelectric material production. The *p*- and *n*-doped semiconductors were then sintered at 580°C with a pressure of approximately 50 MPa using an electric current-assisted sintering press as described for use with other materials in<sup>11</sup> to form pellets of 50 mm diameter and a suitable height. Process parameters and holding times were adjusted to obtain an optimal density. The pellets were then cut into semiconductor legs using a high-speed wafer dicing saw.

Samples of appropriate sizes were also manufactured to characterise the thermoelectric properties of the materials produced. A measurement facility for high-temperature characterisation of electrical conductivity and the Seebeck coefficient available at DLR,<sup>12</sup> and a laser flash method for thermal diffusivity measurements, were used to provide *ZT* data (Fig. 5) for thermoelectric modeling of module design conducted afterwards. The data shown here represent the properties of preliminary skutterudite material that show a lower *ZT* than reported elsewhere. An optimization of the materials' properties was not intended in the context of the work presented in the paper. Materials were chosen due to their similarity between *n*- and *p*-type material which allowed omitting an adjustment of the legs' cross-sections relative to each other in the module's design. The data was then used for modeling the TEM.

## DEVELOPMENT OF A THERMOELECTRIC MODULE SUITABLE FOR VEHICLE APPLICATIONS

### Underlying Layer Sequence

A layer sequence for the structure of a positively-bonded module design has been developed at DLR against a background of later series production,

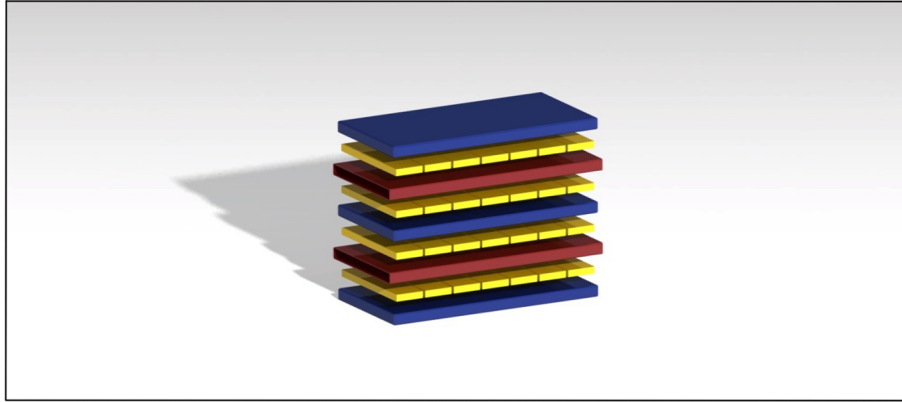


Fig. 3. Schematic view of a TEG layered compound structure with hot side heat exchanger (red), cooling water heat exchanger (blue) and thermoelectric modules (yellow) (Color figure online).



Fig. 4. DLR's facility for thermoelectric material production.

high efficiency and integration into TEGs suitable for vehicles.<sup>13</sup> Figure 6 is a diagrammatic representation of the sequence of layers

The application of an electrical insulating layer (yellow) to a metallic substrate (heat exchanger or sheet metal; light grey) with the greatest possible heat conductivity and minimal layer thickness is anticipated. The electrical bridges shown in dark grey are also intended to have low layer thicknesses, to minimize the temperature gradients from the heat source to the thermoelectric (TE) legs. Finally, the ends of the TE legs can be connected to the electrical bridges by soldering or alternative methods such as diffusion bonding. The symmetrical layer sequence facilitates a reduction in production outlay.

### Plasma-Sprayed Multilayer Films

Analogous to the layer sequence described in the previous section, stainless steel (1.4301) was selected as the substrate for the experiments described here. An electrically-insulating layer of  $MgAl_2O_4$  was applied to it by plasma spraying. A

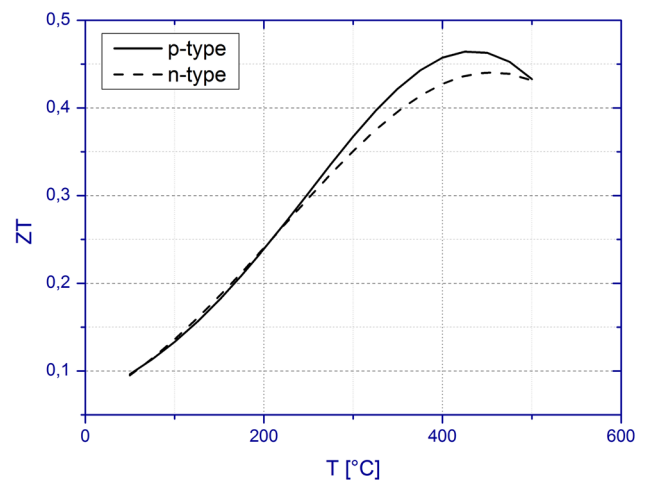


Fig. 5.  $ZT$  of preliminary skutterudite materials used for modeling; similarity between  $n$ - and  $p$ -type material allowed omitting an adjustment of the legs' cross-sections relative to each other in the module's design.

gradient layer of nickel and silver was used to produce the electrical bridges, in order to facilitate subsequent bonding by pressure sintering. Figure 7 is a diagrammatic representation of the procedure for coating the metal substrate.

In the first step, the substrate is coated with spinel. The hot and cold side layouts of the electrically-conductive bridges are then applied, using coating masks. The semiconductor legs are also coated with the bridge material, which consists of a nickel and silver gradient layer. This process has to be repeated for the top and underside of the legs. The final step is the bonding of the module, in which the individually-produced components are joined under pressure and temperature.

The left-hand illustration in Fig. 8 shows a coated substrate for the hot side of the module. The right-hand image in Fig. 8 is a scanning electron microscopy (SEM) image of a layer with  $\times 500$  magnification. The very dense grey substrate is stainless steel, to which spinel is applied. Spinel

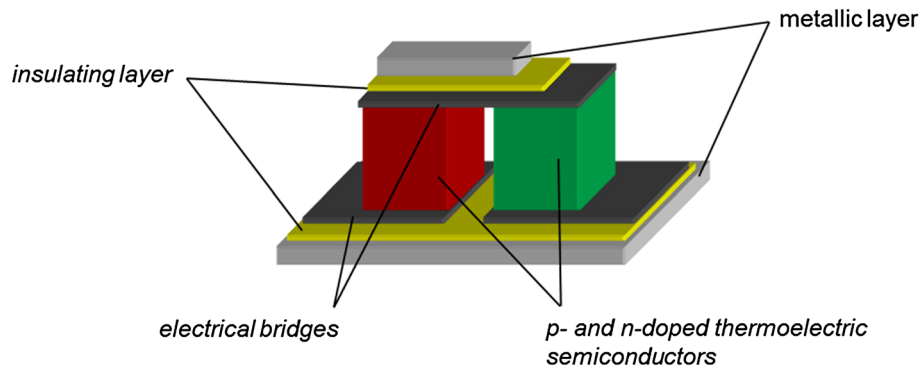


Fig. 6. Layer sequence developed for the structure of TEMs suitable for vehicles.

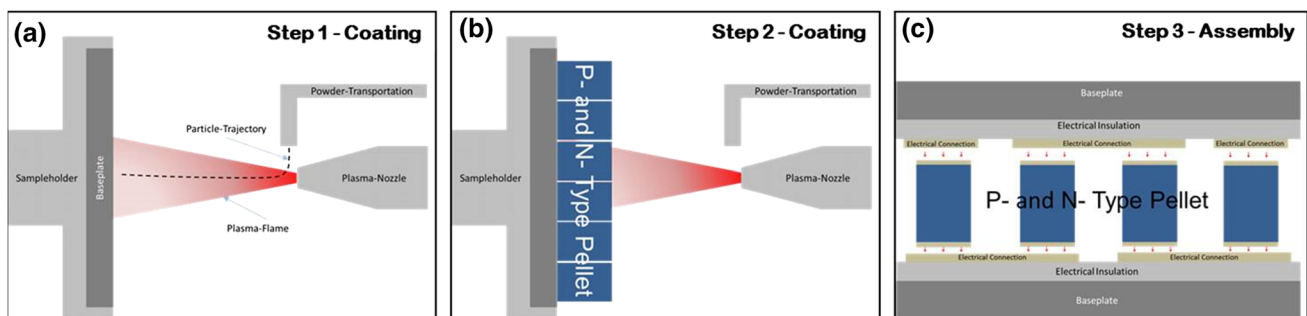


Fig. 7. Diagrammatic representation of the process for coating and subsequent bonding, (a) Step 1 – coating the baseplate, (b) Step 2 – coating the TE material, (c) Step 3 – assembly by diffusion bonding.

displays very good, firm layer bonding to the stainless steel. Few air inclusions and a lamellar structure of the sprayed-on layer are evident. The spinel is followed by the bridge material, applied as a gradient-layer coating. Two shades of grey are discernible in the layer, representing silver (light) and nickel (dark). The proportion of silver increases as the layer thickens. It thus increases from 50% to 100% in the uppermost layer. Such a combination of layers serves adjustment of the coefficients of thermal expansion and better bonding in the next step. The high proportion of silver on the short surfaces or leg contact points is intended to facilitate bonding by pressure sintering.

### Simulative Design of a Thermoelectric Module Using a Constant-Property Model and the FEM

As temperature-dependent material properties, boundary and working conditions are given, the theoretical thermodynamic potential of the performance of a thermoelectric module, i.e. the power output (density) and the efficiency, can be determined for the particular situation of installation. The design of a module has to be matched to achieve optimum performance in respect of these constraints and conditions. One key parameter in the design of a TEM and control of its performance is the length of the legs.<sup>14–18</sup> Having fixed both the temperatures at

the hot and cold side and the ingoing heat flux, a unique length has to be calculated. The leg length depends on numerous parameters, besides the material properties and the conditions, which can drastically change the performance, e.g. the contacts and corresponding electrical and thermal contact resistances, the packing factor and filling material between the legs.<sup>19</sup> Conceptual requirements for an automotive TEG design were pointed out in “[Vehicle-specific boundary conditions](#)”. These requirements result in special conditions and constraints serving as a basis for the determination of the leg length of TE elements to achieve optimum performance. Three distinct steps are used to calculate the leg length:

1. The constant properties model (CPM) is used to narrow down the parameter space. In this classical one-dimensional method, only the TE thermocouple is considered, without any peripherals, and calculated analytically.
2. Based on this analytical calculation, the next step is to take into account the influence of the peripherals (metallic bridges, insulation, supporting structure). This semi-analytical calculation prepares the final step, a finite element analysis.
3. Finally, a finite element method (FEM) calculation comprising the system with all its layers in a real three-dimensional structure is used to calculate the leg length for the given conditions in

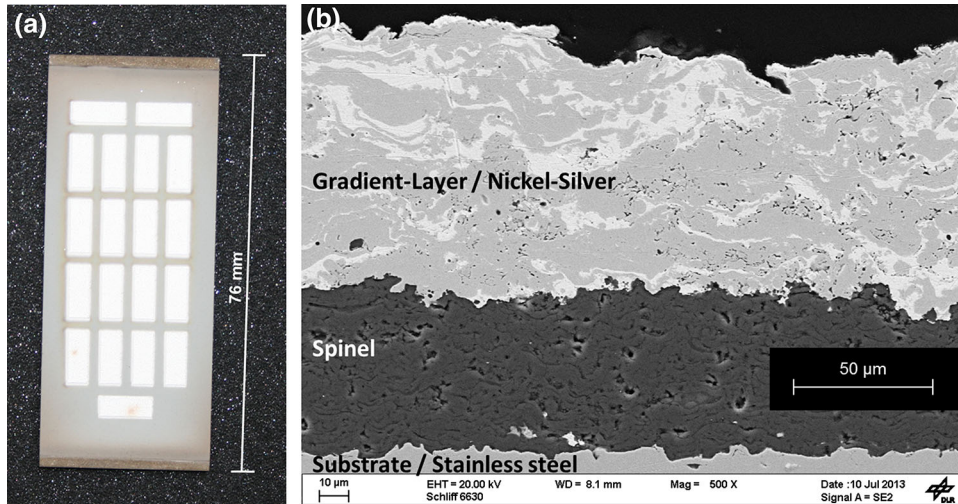


Fig. 8. (a) coated substrate for the hot side of the module; (b) scanning electron microscopy image of the nickel and silver gradient layer.

the parameter space previously defined. For this purpose, a thermocouple (*p*-type/*n*-type leg with bridges, insulation and support) is taken as the base unit for the calculation (Fig. 9). Optimum performance for this thermocouple is determined and, based on that, scaled up for the module.

In Fig. 9, the local temperature distribution calculated by FEM for the given conditions and a current of  $I = 2$  A is shown. The performance of the module (power output and efficiency) depending on the load (the corresponding current) is determined in the knowledge of the temperature field and the electrical potential. Two cross-sectional areas of elements, which result in two different packing rates for the module, were investigated in detail. For manufacturing and handling reasons, the larger cross-sectional area was chosen and the length varied for the TE elements to fulfill the conditions and constraints. Under ideal conditions, the optimum power output for one module unit (62 mm × 26 mm, 19 base units as in Fig. 8a) in this design is then approximately 15 W.

### Thermomechanical Calculations of Material Stability

Further work on mechanical stability is necessary, in addition to thermoelectric design calculations. One major challenge is the guarantee of long-term stable thermal conductivity between the thermoelectric modules and the heat exchanger and within the laminar structure, despite local temperature gradients and different material properties. Thermomechanical simulation is therefore crucial to identify low-stress structural configurations in the development of promising module designs.

For this purpose, thermally- and mechanically-induced stresses were calculated on the basis of FEM simulations (Ansys). An FEM model was constructed in accordance with specified geometrical

variables and material properties, and subjected to thermal and mechanical conditions. Suitable contact elements were used to represent the contact process in the functional laminated structure. After meshing in resolution dictated by the geometry and the iterative solution process, the stress-dependent results allow statements on local material stresses and on stability limits.

Using the example of the laminated structure determined in “[Underlying Layer Sequence](#)”, structural mechanical simulations were carried out for which a hot side temperature of 550°C and a cold side temperature of 110°C were specified. The distribution of stress is shown in Fig. 10.

The resultant temperature profile produces thermal expansion of the structure and thus tensile stresses in the functional laminated structure. High local tensile stresses arise, due to the differences in the coefficient of thermal expansion attributable to the material. This is particularly evident in the electrical insulation on the hot side (above), where the high differences in temperature and the low coefficients of thermal expansion compared to the surrounding metallic layers produce high tensile stresses of up to 150 MPa. The stresses determined in the exemplarily functional laminated structure indicate stability problems inside the electrical insulation and thus risks in a long-term stable structure.

The results of the simulation show clearly that thermomechanical aspects are crucial to the development of efficient, durable functional laminated structures. The simulation model developed here allows the identification of TEG modules with long-term stability by variations in the material and geometry. Continuing work is primarily focused on improved representational accuracy between the surrounding heat exchanger and the TEG modules, with the objective of designing self-reinforcing structures and thus stable composite structures.

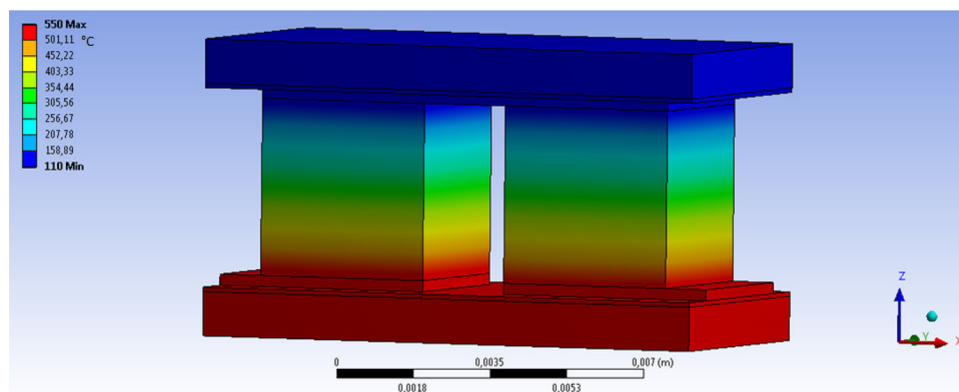


Fig. 9. FEM result for temperature distribution in the base unit of a TE module ( $T_h = 550^\circ\text{C}$ ,  $T_c = 110^\circ\text{C}$ ,  $I = 2\text{A}$ ).

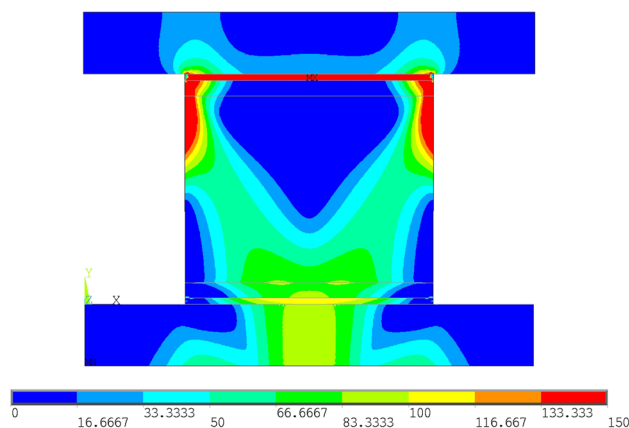


Fig. 10. Distribution of stress in the exemplarily functional laminated structure in MPa.

## CONCLUSION AND OUTLOOK

The investigations described here reveal a possible design for the structure of TEMs suitable for vehicles. An elongated module design with a planar structure displaying low thermal surface transfer impedances was derived from the system requirements and conditions. The following were used:

- Metallic substrate
- Plasma-sprayed thin insulation— $\text{MgAl}_2\text{O}_4$
- Plasma-sprayed bridge-gradient nickel and silver layer
- Joining by diffusion bonding

Initial trials produced a very good, strong bond between the insulation layer and the stainless steel, with few air inclusions and a lamellar structure. The bridge material applied in the form of multiple layers also displayed the anticipated layer pattern. It was possible to successfully demonstrate the parallel development of a process for the series production of skutterudite-based TE material by using a gas stream. Figures-of-merit ( $ZT$ ) of approximately 0.4 were achieved for  $n$ - and  $p$ -doped material. The thermoelectrical and mechanical simulations carried out displayed high energetic potential (15 W output

at  $62\text{ mm} \times 26\text{ mm}$ ), but conversely presented major challenges in terms of long-term stability. Continuing work will concentrate on experimental trials, i.e. the practical implementation of the concept presented. An additional focus will be on the reduction of thermally-induced stresses in the laminar TEM structure. Module-specific electrical power extraction by MPPT will also form part of future research projects.

## REFERENCES

1. B. Propfe, and D. Luca de Tena, Perspectives of electric vehicles: customer suitability and renewable energy integration. *Conference Proceedings. The 25th World Battery, Hybrid and Fuel Cell Electric Vehicle Symposium Exhibition (EVS 25)*, (Shenzhen, China, November 5–9, 2010).
2. D. Jansch (ed.), *Thermoelectrics goes automotive: Thermoelektrik II*, expert 2010.
3. D. Jansch (ed.), *Thermoelectrics Goes Automotive II: Thermoelektrik, III*, expert 2012.
4. J. Yang, *J. Electron. Mater.* 38, 1245 (2009). doi:10.1007/s11664-009-0680-z.
5. M. Kober, C. Häfele, H.E. Friedrich (2012) 3 *International Conference 'Thermoelectrics goes Automotive'* (Berlin, November 21–23 2012).
6. K. Ikoma, M. Munekiyo, K. Furuya, M. Kobayashi, T. Izumi, and K. Shinohara, Thermoelectric Module and Generator for Gasoline Engine Vehicle. *Proceedings of 17th International Conference on Thermoelectrics*, IEEE (Nagoya, Japan, 1998) p. 464. doi: 10.1109/ICT.1998.740419.
7. E.F. Thacher, B.T. Helenbrook, M.A. Karri, and J. Richter Clayton, *Proc. Inst. Mech. Eng. D* 2212007, 95 (2007). doi:10.1243/09544070JAUTO51.
8. T. Ochi, et al., *J. Electron. Mater.* 43, 2344 (2014). doi:10.1007/s11664-014-3060-2.
9. M. Klein Altstedde, F. Rinderknecht, and H. Friedrich, *J. Electron. Mater.* 43, 2134 (2014). doi:10.1007/s11664-014-2990-z.
10. J. Fleuriel, T. Caillat, and A. Borshchevsky, *Skutterudites: a new class of promising thermoelectric materials. XIII International Conference on Thermoelectrics* (Kansas City, MO 1994) p. 40.
11. A. Schmitz, C. Stiewe, and W.E. Müller, *J. Electron. Mater.* 40, 543 (2011). doi:10.1007/s11664-010-1442-7.
12. J. de Boor, et al., *J. Electron. Mater.* 42, 1711 (2013). doi:10.1007/s11664-012-2404-z.
13. J.P. Longtin, L. Zuo, D. Hwang, G. Fu, M. Tewolde, Y. Chen, and S. Sampath, *J. Thermal Spray Technol.* 22, 577 (2013).

14. S.J. Angello, C.J. Frank, J.D. Meess, P.H. Sutter, and G.W. Wilson, Technology of thermoelectric devices. *Thermoelectricity. Science and Engineering*, ed. R.R. Heikes and R.W. Ure, Jr (New York: Interscience Publishers, 1961), .
15. A.F. Ioffe, *Semiconductor Thermoelements and Thermoelectric Cooling* (London: Infosearch Limited, 1957).
16. Min Gao, Thermoelectric Module Design Theories. *Thermoelectrics Handbook. Macro to Nano*, ed. D. Mike Rowe (Boca Raton: CRC Taylor & Francis, 2006), p. 11-1.
17. Gerhard C. Stoll, Robert L. Eichorn, and Richard G. Sickert, Thermoelectric Device Design. *Thermoelectricity*, ed. Paul H. Egli (New York: Wiley, 1960), p. 30.
18. R.W. Ure Jr. and R.R. Heikes, Theoretical Calculation of Device Performance. *Thermoelectricity. Science and Engineering*, ed. R.R. Heikes and R.W. Ure (New York: Interscience, 1961), p. 458.
19. P. Ziolkowski, P. Poinas, J. Leszczynski, G. Karpinski, and E. Müller, *J. Electron. Mater.* 39, 1934 (2010). doi:[10.1007/s11664-009-1048-0](https://doi.org/10.1007/s11664-009-1048-0).